

Supporting Information for:
**Suppression of Phosphine-Protected Au₉ Clusters Agglomeration on SrTiO₃
Particles Using a Chromium Hydroxide Layer**

Abdulrahman S. Alotabi^{1,2,3}, D. J. Osborn⁴, Yuki Kataoka⁵, Shuhei Ozaki⁵, Yuichi Negishi⁵,
Siriluck Tesana⁶,
Gregory F. Metha⁴ and Gunther G. Andersson^{1,3*}

¹ Flinders Institute for Nanoscale Science and Technology, Flinders University, Adelaide, South Australia 5042, Australia

² Department of Physics, Faculty of Science and Arts in Baljurashi, Albaha University, Baljurashi 65655, Saudi Arabia

³ Flinders Microscopy and Microanalysis, College of Science and Engineering, Flinders University, 5042 Adelaide, Australia

⁴ Department of Chemistry, University of Adelaide, Adelaide, South Australia 5005, Australia

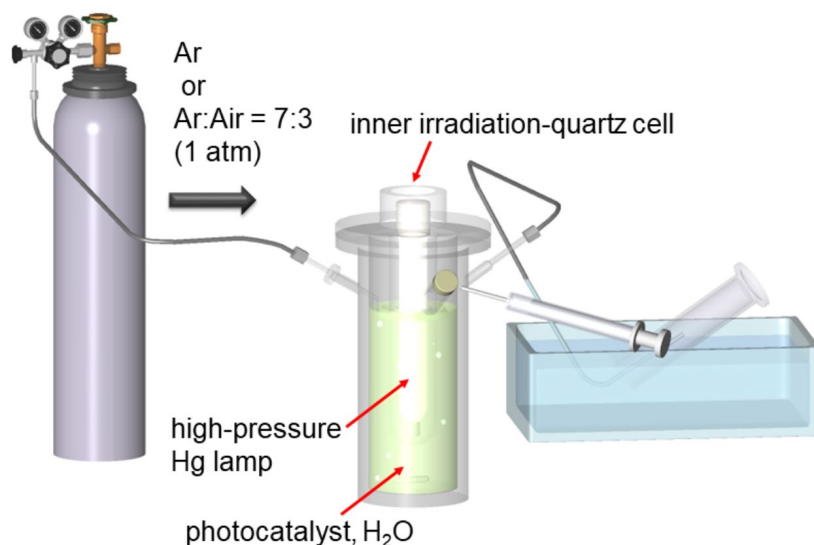
⁵ Department of Applied Chemistry, Faculty of Science, Tokyo University of Science, 1-3 Kagurazaka, Shinjuku-ku, Tokyo 162-8601, Japan

⁶ The MacDiarmid Institute for Advanced Materials and Nanotechnology, School of Physical and Chemical Sciences, University of Canterbury, Christchurch 8141, New Zealand

Analytical Methods:

- X-ray diffraction (XRD)

XRD patterns were recorded with an irradiation source of Co-K α ($\lambda = 1.789 \text{ \AA}$) at 35 kV and 28 mA using a Bruker D8 diffractometer over a 2θ range of 20° to 60° .

ADDITIONAL FIGURES

Scheme S1: Schematic of the measurement of the photocatalytic activity in this study. Ref. ¹.

Copyright 2018 American Chemical Society.

Figure S1 shows the Sr 3d and P 2p spectra of SrTiO₃ and SrTiO₃-Au₉ before and after heating. The Sr 3d_{5/3} peak for SrTiO₃ appeared at a binding energy of 133.6 eV. The significant intensity of the Sr 3d peak overlapped with the P 2p region, which meant that it was more difficult to fit and determine the chemical state of triphenylphosphine ligands.

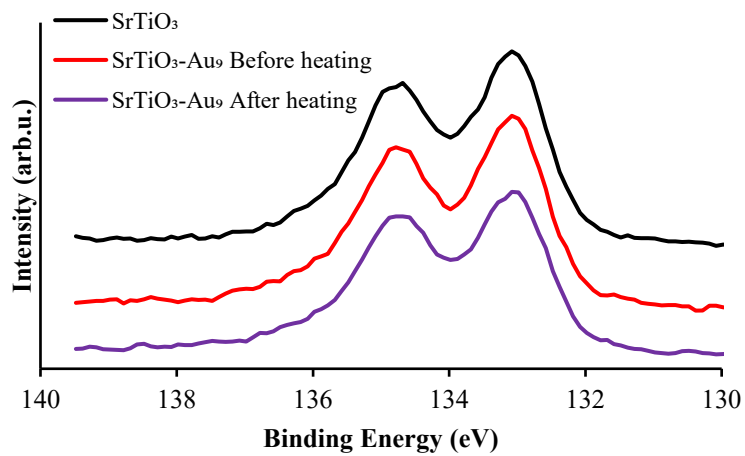


Figure S1: XPS Sr 3d and P 2p spectra of SrTiO₃ and SrTiO₃-Au₉ before and after heating

Effect of high-energy STEM electron beam irradiation on Au₉ clusters.

Figure S2 shows HAADF-STEM images after successive EDX elemental mapping measurements. These images show the effect of the high-energy STEM electron beam on the Au₉ clusters at the surface. Drift and agglomeration of Au₉ clusters were observed; the former is attributed to heating of the sample and the latter to beam damage. This effect must be considered for the size analysis of Au clusters from STEM-HAADF and the STEM EDX elemental mapping data.

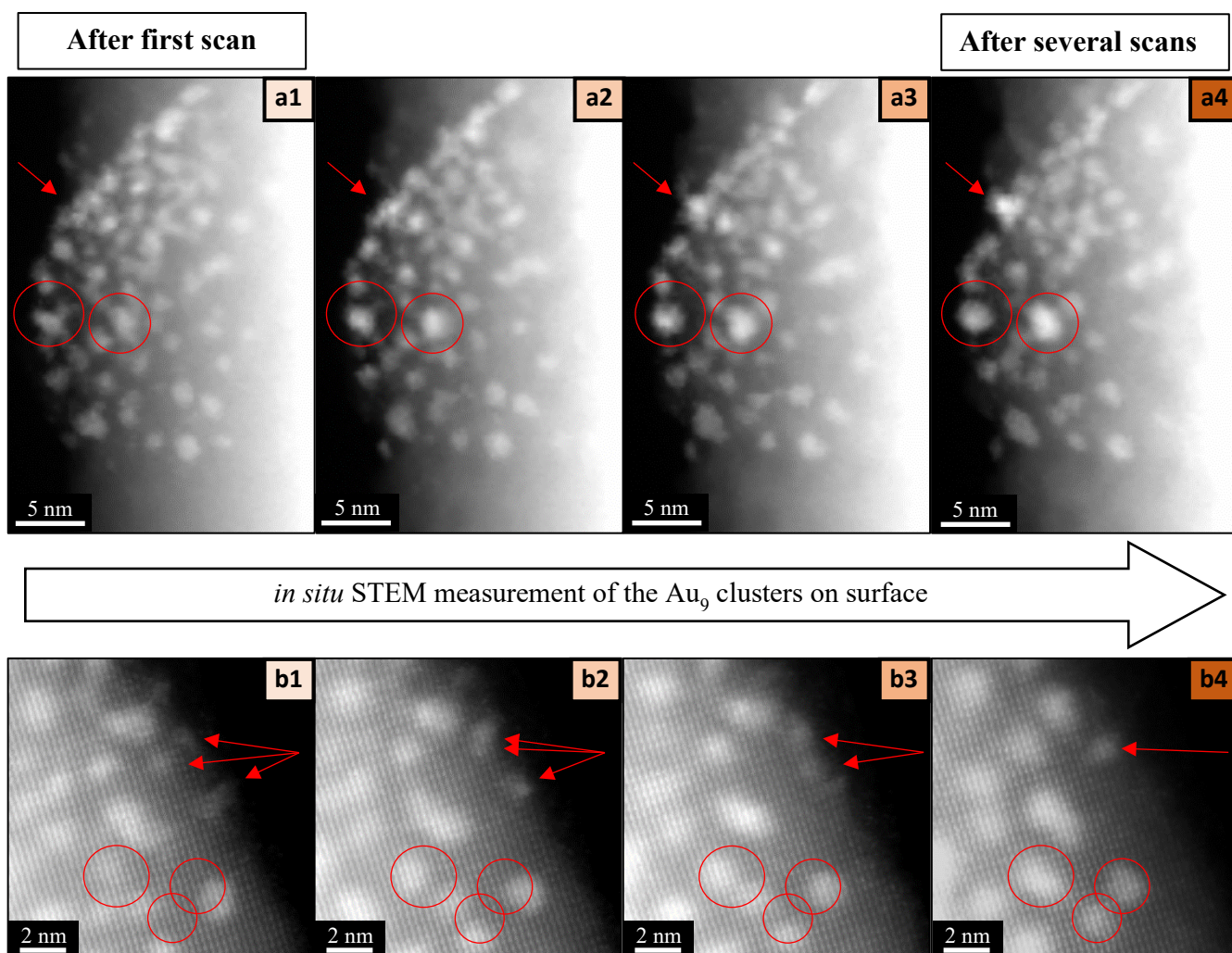


Figure S2: HAADF-STEM images of *in situ* STEM measurements of the Au₉ clusters on SrTiO₃-Au₉-Cr(OH)₃ before heating (a and b). The images display after the first and several scans with red circles and arrows indicated the clusters damaged by the STEM electron beam.

Figure S3 shows the Ba 3d spectrum of SrTiO₃-Au₉ after heating. The binding energy of Ba 3d_{5/2} appears at 780.5 ± 0.2 eV corresponding to Ba metal. The presence of barium in the SrTiO₃-Au₉

sample due to the commercial contamination of SrTiO₃ (99%, Sigma-Aldrich). Using XPS relative intensity, the amount of barium contamination is approximately < 1%.

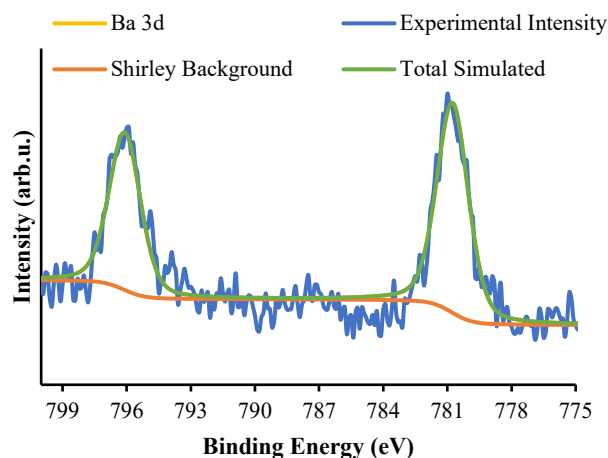


Figure S3: XPS Ba 3d spectrum of SrTiO₃-Au₉ after heating.

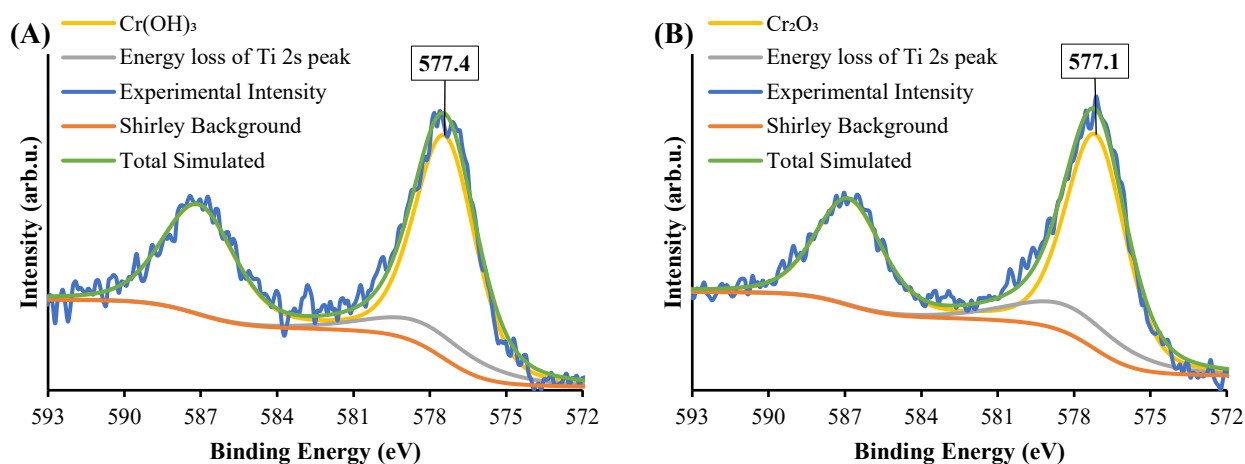


Figure S4: XPS Cr 2p spectra of (A) SrTiO₃-Au₉ after photodeposition of a CrO_x layer and (B) after heating.

Figure S5 shows the H₂ production after 1 h irradiation using 10% methanol as a sacrificial reagent under two conditions: (1) using Ar gas flow during the irradiation (without O₂) and (2) using Ar gas and air (7:3) mixture flow during the irradiation (with O₂) to investigate the back reaction process. For SrTiO₃ and SrTiO₃-Au₉, the level of H₂ production reduced by a factor of two after introducing air into the reactor. This was due to the recombination of H₂ and O₂ (from air) to water, which reduces the H₂ evaluation reaction. For SrTiO₃-Au₉ with a Cr(OH)₃ layer, the level of H₂ production did not

show a significant reduction after introducing air into the reactor, which indicated that $\text{Cr}(\text{OH})_3$ inhibited the back reaction.

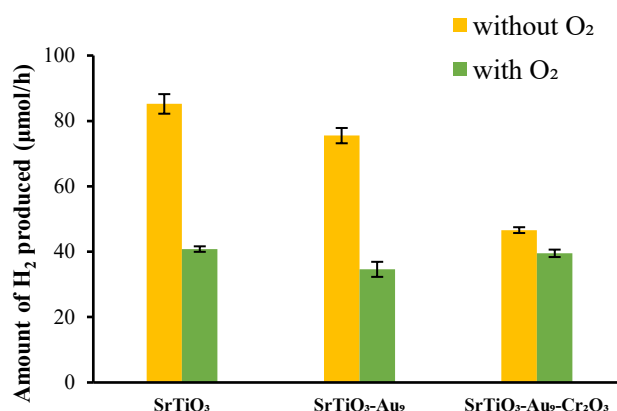


Figure S5: Comparison of the H_2 evolution reactions of SrTiO_3 , $\text{SrTiO}_3\text{-Au}_9$ and $\text{SrTiO}_3\text{-Au}_9\text{-Cr}(\text{OH})_3$ using 10% methanol as a sacrificial reagent under flow of Ar gas (without O_2) and flow of Ar and air 7:3 mixture (i.e. with O_2). The values are average of two hours irradiation.

Table S1: XPS Au $4f_{7/2}$ peak positions, full width at half maximum (FWHM) and relative HBP:LBP intensities with the size of Au features from STEM.

	SrTiO ₃ -Au ₉				SrTiO ₃ -Au ₉ -Cr(OH) ₃			
	Peak position (eV)	FWHM	Intensity %	HAADF-STEM Size of Au features	Peak position (eV)	FWHM	Intensity %	HAADF-STEM Size of Au features
Before heating								
HBP	84.8 ± 0.2	1.8 ± 0.2	83	0.7–1.3 nm	85.0 ± 0.2	1.9 ± 0.2	90	1.3–1.6 nm
LBP	84.1 ± 0.2	1.2 ± 0.2	17		84.1 ± 0.2	1.2 ± 0.2	10	
After heating								
HBP	85.4 ± 0.2	2.0 ± 0.2	50	-	84.9 ± 0.2	2.0 ± 0.2	65	-
LBP	83.7 ± 0.2	1.2 ± 0.2	50		83.8 ± 0.2	1.2 ± 0.2	35	
After 7 h irradiation								
HBP	85.2 ± 0.2	2.2 ± 0.2	30	3.9–6.9 nm	84.9 ± 0.2	2.2 ± 0.2	63	1.4–2.7 nm
LBP	83.5 ± 0.2	1.2 ± 0.2	70		83.9 ± 0.2	1.2 ± 0.2	37	

Table S2: XPS peak positions of SrTiO₃-Au₉ and SrTiO₃-Au₉ after photodeposition of a Cr(OH)₃ layer.

Sample \ Element	C 1s			Au 4f _{7/2}		Sr 3d _{5/2}	Ti 2p _{3/2}	O 1s		Ba 3d _{5/2}	Cr 2p _{3/2}
	P1	P2	P3	HBP	LBP	P1	P1	P1	P2	P1	P1
SrTiO₃-Au₉											
Before heating	285	286.0	---	84.8	84.1	133.0	458.6	531.8	529.7	780.3	---
After heating	285	285.7	290.7	85.4	83.7	133.3	458.8	531.8	529.9	780.5	---
After photocatalysis	285	285.8	290.1	85.2	83.5	133.2	458.7	531.6	529.9	780.5	---
SrTiO₃-Au₉-CrO_x											
Before heating	285	286.4	289.8	85.0	84.1	133.0	458.5	531.6	529.7	780.4	577.4
After heating	285	290.5	---	84.9	83.8	133.1	458.6	531.4	529.8	780.1	577.1
After photocatalysis	285	285.7	289.8	84.9	83.9	133.2	458.7	531.5	529.9	780.4	577.5

* P1: Peak 1

**HBP: High binding peak. LBP: Low binding peak

Table S3: XPS elemental composition of SrTiO₃-Au₉ and SrTiO₃-Au₉ after photodeposition of a Cr(OH)₃ layer.

Sample \ Element	C 1s			Au 4f _{7/2}		Sr 3d _{5/2}	Ti 2p _{3/2}	O 1s		Ba 3d _{5/2}	Cr 2p _{3/2}
	P1	P2	P3	HBP	LBP	P1	P1	P1	P2	P1	P1
SrTiO₃-Au₉											
Before heating	10.81	2.15	---	0.54	0.11	12.32	13.48	23.77	36.58	0.24	---
After heating	7.12	2.50	1.01	0.17	0.17	13.10	13.62	23.36	38.47	0.47	---
After photocatalysis	6.31	2.37	1.09	0.07	0.16	14.28	14.09	19.12	41.96	0.56	---
SrTiO₃-Au₉-CrO_x											
Before heating	8.78	2.01	1.22	0.21	0.02	10.59	10.66	31.33	29.42	0.35	5.41
After heating	6.97	1.36	---	0.13	0.07	11.99	12.02	28.19	33.97	0.24	5.06
After photocatalysis	5.64	3.85	0.54	0.12	0.07	11.72	10.86	31.47	30.39	0.20	5.15

* P1: Peak 1

**HBP: High binding peak. LBP: Low binding peak

Table S4: Summary of Cr 2p_{3/2} peak position of various samples.

Sample	Cr 2p _{3/2} peak position (eV)
Cr ₂ O ₃	576.9 ± 0.2
Cr(OH) ₃	577.5 ± 0.2
SrTiO ₃ -Cr(OH) ₃	577.6 ± 0.2
SrTiO ₃ -Au ₉ -Cr(OH) ₃	577.4 ± 0.2
SrTiO ₃ -Au ₉ -Cr ₂ O ₃ heated	577.1 ± 0.2
SrTiO ₃ -Au ₉ -Cr(OH) ₃ after 7 h irradiation	577.5 ± 0.2
SrTiO ₃ -Au ₉ -Cr ₂ O ₃ after irradiation (without O ₂)	577.5 ± 0.2
SrTiO ₃ -Au ₉ -Cr ₂ O ₃ after irradiation (with O ₂)	577.5 ± 0.2

XPS Au 4f spectra of SrTiO₃-Au₉ and SrTiO₃-Au₉-Cr(OH)₃ after irradiation during water splitting reaction for without O₂ and with O₂ samples are shown in Figure S6. Table S5 showed a summary of the Au 4f peak positions and FWHM. A full elemental composition analyses and peak positions are presented in Tables S6 and S7. The Au 4f spectrum for SrTiO₃-Au₉ without O₂ was fitted with 59% of the intensity at HBP (84.9 ± 0.2 eV with an FWHM of 2.0 ± 0.2 eV) corresponding to Au clusters and 41% agglomerated clusters at LBP (83.6 ± 0.2 eV with an FWHM of 1.2 ± 0.2 eV) (Figure S6A). As shown in Figure S6B, for SrTiO₃-Au₉ with O₂, the Au 4f spectrum was fitted with 26% and 74% at HBP(84.9 ± 0.2 eV with an FWHM of 2.0 ± 0.2 eV) and LBP (83.5 ± 0.2 eV with an FWHM of 1.2 ± 0.2 eV), which represented the non-agglomerated and agglomerated clusters. In Figure S6C, the HBP and LBP of Au 4f_{7/2} SrTiO₃-Au₉-Cr(OH)₃ without O₂ were observed at 85.1 ± 0.2 eV (62%) and 84.0 ± 0.2 eV (38%) with an FWHM of 2.0 ± 0.2 eV and 1.2 ± 0.2 eV, respectively. In Figure S6D, with O₂, the HBP and LBP were observed at 84.9 ± 0.2 eV (55%) and 83.9 ± 0.2 eV (45%) with an FWHM of 2.0 ± 0.2 eV and 1.2 ± 0.2 eV, respectively. In SrTiO₃-Au₉-Cr(OH)₃ catalyst, more than a half of the Au clusters were stable at the surface of SrTiO₃ in the present experiment (without and with O₂). This demonstrated that the Cr(OH)₃ helped inhibit the agglomeration of Au₉ clusters during the water splitting reaction with a sacrificial reagent (10% methanol).

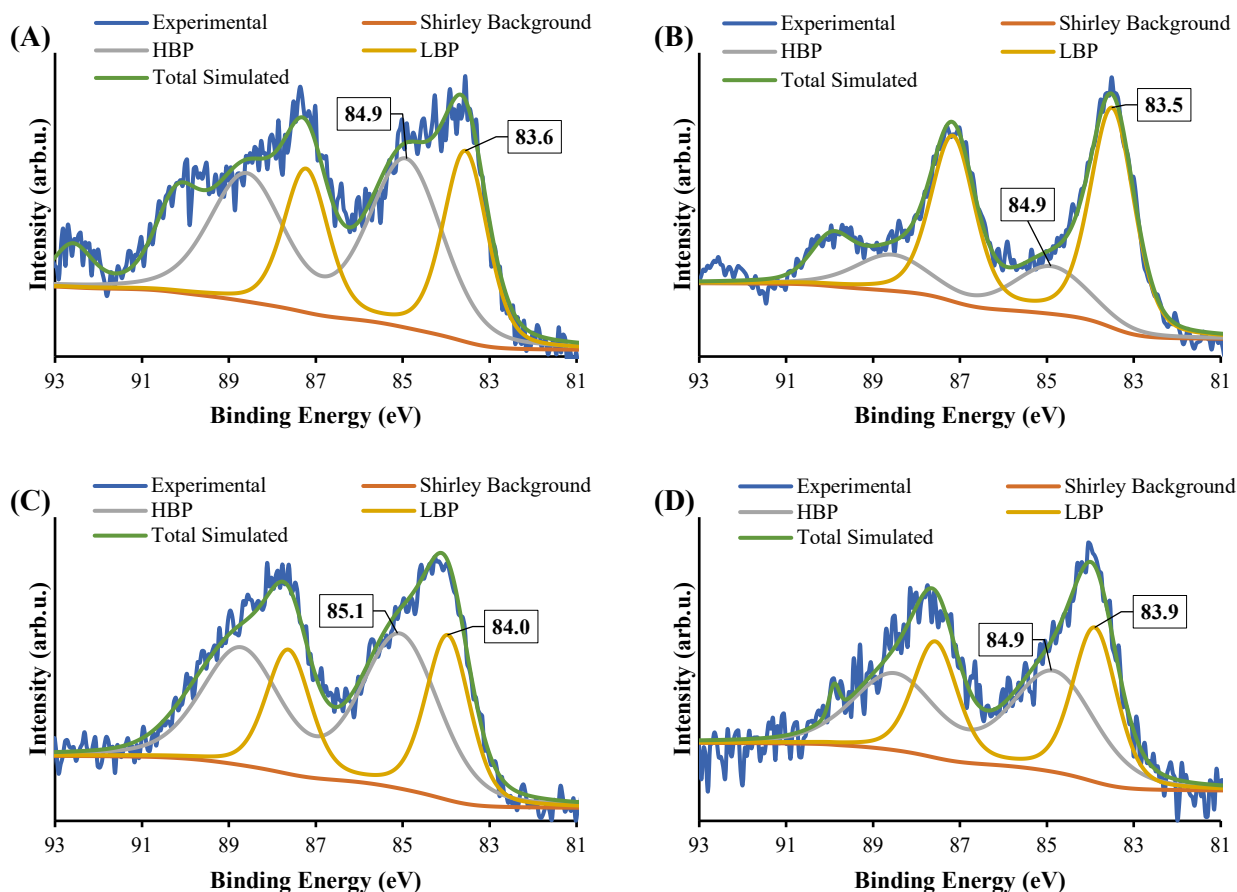


Figure S6: XPS spectra of Au 4f of SrTiO₃-Au₉ after photocatalytic water-splitting reaction with (A) 10% CH₃OH (without O₂), and (B) 10% CH₃OH + (7:3 Ar:air) mixture (with O₂). (C) SrTiO₃-Au₉-Cr(OH)₃ after photocatalytic water-splitting reaction with 10% CH₃OH (without O₂), and (D) 10% CH₃OH + (7:3 Ar:air) mixture (with O₂).

Table S5: XPS Au 4f_{7/2} peak positions, FWHM and relative HBP:LBP intensities.

	SrTiO ₃ -Au ₉			SrTiO ₃ -Au ₉ -Cr(OH) ₃		
	Peak position (eV)	FWHM	Intensity %	Peak position (eV)	FWHM	Intensity %
After photocatalysis (without O₂)						
HBP	84.9 ± 0.2	2.0 ± 0.2	59	85.1 ± 0.2	2.1 ± 0.2	62
LBP	83.6 ± 0.2	1.2 ± 0.2	41	84.0 ± 0.2	1.2 ± 0.2	38
After photocatalysis (with O₂)						
HBP	84.9 ± 0.2	2.0 ± 0.2	26	84.9 ± 0.2	2.2 ± 0.2	55
LBP	83.5 ± 0.2	1.2 ± 0.2	74	83.9 ± 0.2	1.2 ± 0.2	45

Table S6: XPS peak positions of SrTiO₃-Au₉ and SrTiO₃-Au₉ after photodeposition of a Cr(OH)₃ layer.

Sample \ Element	C 1s			Au 4f _{7/2}		Sr 3d _{5/2}	Ti 2p _{3/2}	O 1s		Ba 3d _{5/2}	Cr 2p _{3/2}
	P1	P2	P3	HBP	LBP	P1	P1	P1	P2	P1	P1
SrTiO₃-Au₉											
After photocatalysis (without O ₂)	285	286.1	---	84.9	83.6	134.8	460.3	533.1	531.4	781.8	---
After photocatalysis (with O ₂)	285	285.6	290.4	84.9	83.5	133.3	458.8	531.6	530.0	780.5	---
SrTiO₃-Au₉-CrO_x											
After photocatalysis (without O ₂)	285	285.7	---	85.1	84.0	133.2	458.8	531.7	529.9	780.4	755.5
After photocatalysis (with O ₂)	285	285.9	289.5	84.9	83.9	133.2	458.8	531.7	529.9	780.3	577.5

* P1: Peak 1

**HBP: High binding peak. LBP: Low binding peak

Table S7: XPS elemental composition of SrTiO₃-Au₉ and SrTiO₃-Au₉ after photodeposition of a Cr(OH)₃ layer.

Sample \ Element	C 1s			Au 4f _{7/2}		Sr 3d _{5/2}	Ti 2p _{3/2}	O 1s		Ba 3d _{5/2}	Cr 2p _{3/2}
	P1	P2	P3	HBP	LBP	P1	P1	P1	P2	P1	P1
SrTiO₃-Au₉											
After photocatalysis (without O ₂)	5.20	0.27	---	0.19	0.13	15.08	14.87	17.16	46.51	0.60	---
After photocatalysis (with O ₂)	4.37	6.08	0.74	0.07	0.20	13.99	14.29	19.92	39.91	0.43	---
SrTiO₃-Au₉-CrO_x											
After photocatalysis (without O ₂)	7.60	4.65	---	0.14	0.08	11.52	10.44	28.31	31.73	0.16	5.37
After photocatalysis (with O ₂)	3.74	0.87	0.40	0.10	0.09	12.29	11.60	29.87	35.48	0.23	5.32

* P1: Peak 1

**HBP: High binding peak. LBP: Low binding peak

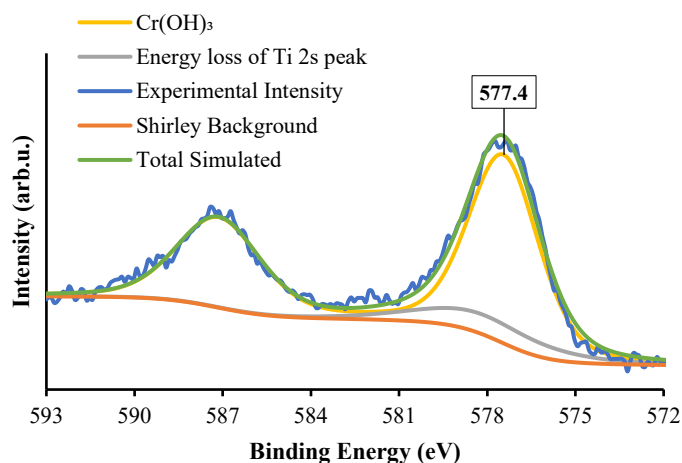


Figure S7: XPS spectrum of Cr 2p of SrTiO₃-Au₉-Cr(OH)₃ after 7 h irradiation.

HAADF-STEM images of SrTiO₃-Au₉ and of SrTiO₃-Au₉-Cr(OH)₃ before heating and after 7 h irradiation are presented in Figure S8 for comparison. As shown in the images, the size of the Au clusters increases up to 8 nm for SrTiO₃-Au₉ after 7 h irradiation due to the aggregation of Au clusters under the ultraviolet (UV) irradiation². However, in terms of SrTiO₃-Au₉-Cr(OH)₃, the Au clusters remain more stable on the surface of SrTiO₃ after 7 h irradiation, up to 2.7 nm.

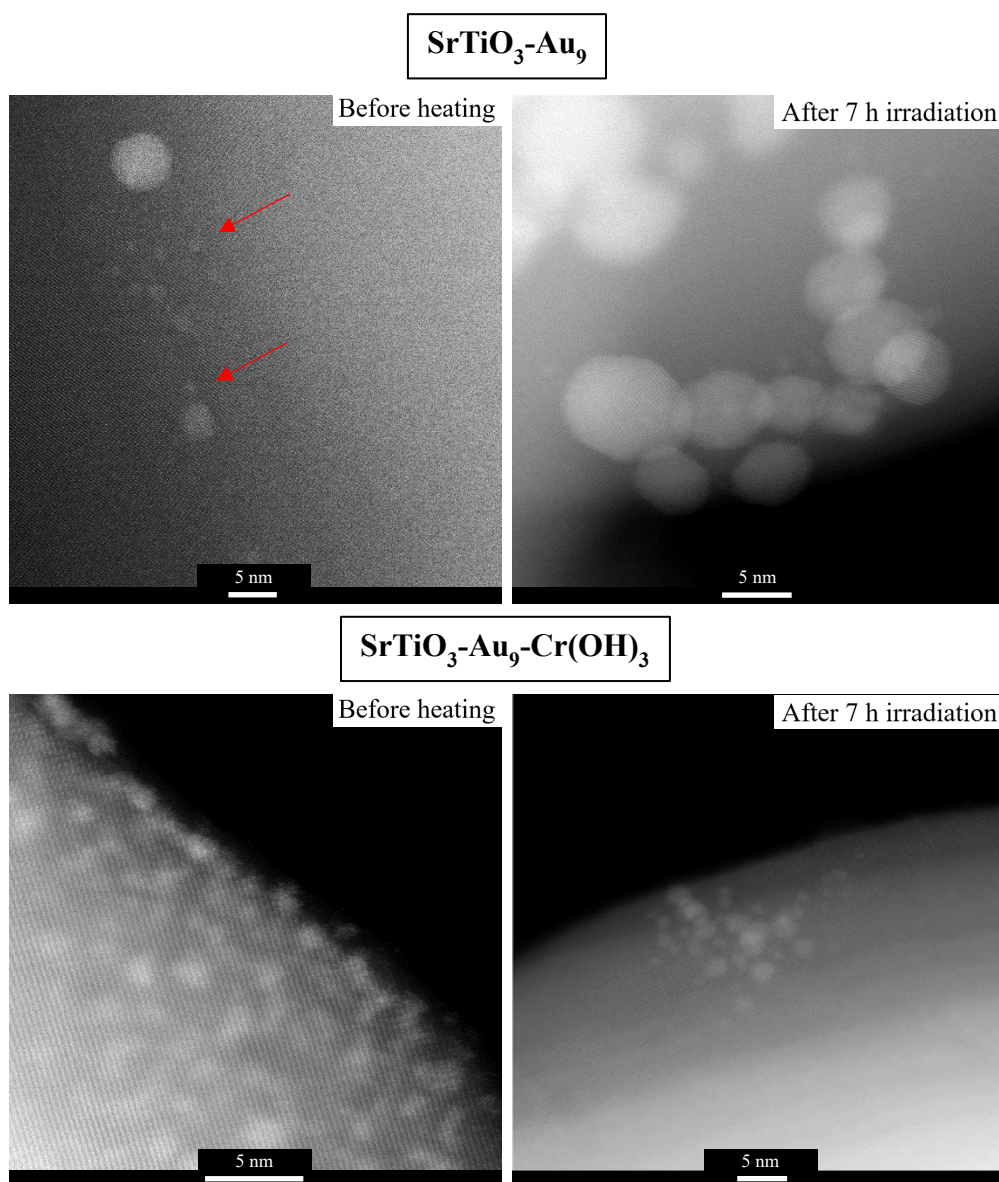


Figure S8: HAADF-STEM images of SrTiO₃-Au₉ and SrTiO₃-Au₉-Cr(OH)₃ before heating and after 7 h irradiation.

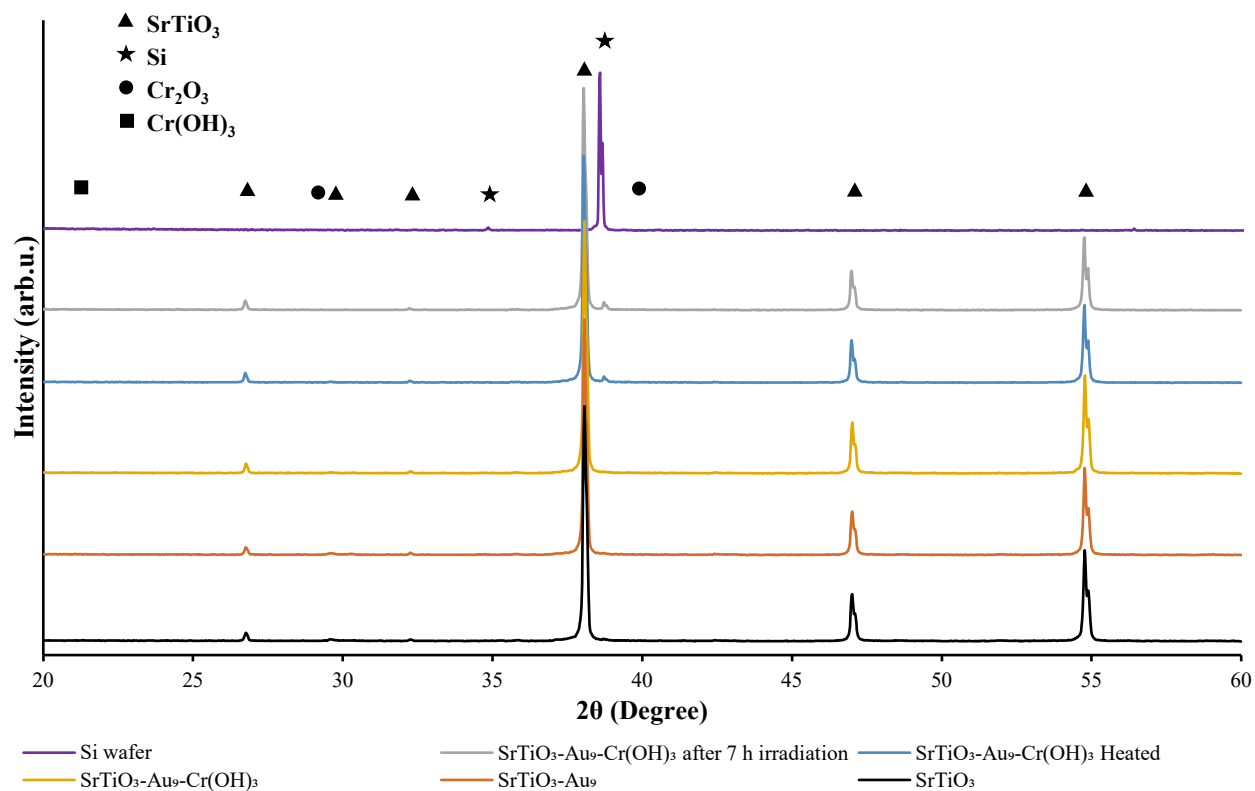


Figure S9 : X-ray diffraction pattern of Si wafer, SrTiO_3 , $\text{SrTiO}_3\text{-Au}_9$, $\text{SrTiO}_3\text{-Au}_9\text{-Cr(OH)}_3$, $\text{SrTiO}_3\text{-Au}_9\text{-Cr}_2\text{O}_3$ heated and $\text{SrTiO}_3\text{-Au}_9\text{-Cr(OH)}_3$ after 7 h irradiation.

REFERENCES

1. W. Kurashige, R. Kumazawa, D. Ishii, R. Hayashi, Y. Niihori, S. Hossain, L. V. Nair, T. Takayama, A. Iwase, S. Yamazoe, T. Tsukuda, A. Kudo and Y. Negishi, *The Journal of Physical Chemistry C*, 2018, **122**, 13669-13681.
2. J.-Y. Ruzicka, F. Abu Bakar, C. Hoeck, R. Adnan, C. McNicoll, T. Kemmitt, B. C. Cowie, G. F. Metha, G. G. Andersson and V. B. Golovko, *The Journal of Physical Chemistry C*, 2015, **119**, 24465-24474.